Fouling during constant flux crossflow microfiltration of pretreated whey. Influence of transmembrane pressure gradient*

Geneviève Gésan-Guiziou, Georges Daufin, Uzi Merin, Jean.-Pierre Labbé, Auguste Quemeraisd

Journal of Membrane Science, 80 (1993) 131–145
Elsevier Science Publishers B V, Amsterdam

Fouling during constant flux crossflow microfiltration of pretreated whey. Influence of transmembrane pressure gradient*

G. Gésan[a], G. Daufin[a,**], U. Merin[b], J.-P. Labbé[c] and A. Quémerais[d]

[a]*Institut National de la Recherche Agronomique, Laboratoire de Recherches de Technologie Laitière, 65, rue de St Brieuc, 35042 Rennes Cédex (France)*

[b]*Agricultural Research Organization, Dairy Science Laboratory, The Volcani Center, PO Box 6, Bet Dagan 50250 (Israel)*

[c]*Ecole Nationale Supérieure de Chimie de Paris, Laboratoire de Corrosion, 11 rue P et M Curie, 75231 Paris Cédex 05 (France)*

[d]*Université Rennes I, Laboratoire de Spectroscopie du Solide, Campus de Beaulieu, 35042 Rennes Cédex (France)*

(Received May 25, 1992, accepted in revised form September 30, 1992)

Abstract

Pretreatment of whey by microfiltration (MF) has emerged as a necessary step in producing high purity whey protein concentrates In the MF of pretreated whey using a Carbosep M14 membrane (pore diameter 0 14 μm), proteins and calcium phosphate aggregates were responsible for fouling, which increased according to the "complete blocking" filtration law and accounted for a progressive decrease of the active filtering area. An operating mode with dynamic counter pressure (recirculation of the permeate co-current to the retentate), as opposed to static counter pressure, allowed lower overall fouling, a longer time of operation and better protein recovery because of more evenly distributed fouling along the membrane tube. At shorter times of operation, fouling was greater under higher transmembrane pressure (TP), so that the less fouled areas under lower TP were forced to filter larger volumes and consequently became fouled more rapidly This involved a movement of the effective filtering area along the membrane tube, as evidenced by the systematic evolution of fouling heterogeneity as measured by infra-red spectroscopy

Keywords microfiltration, whey; fouling; infrared and X-ray photoelectron spectroscopy, hydrodynamics

1. Introduction

Ultrafiltration (UF) of whey for the production of whey protein concentrate (WPC), which has high nutritional and functional properties [1–3], is the major process employed in membrane processing of food. The WPC produced still contains small amounts of residual fat and phospholipids which alter its functionality [4,5]. UF performance during WPC production is altered by membrane fouling. Removal of the major components responsible for such a phenomenon, using pretreatment of the feed streams, has been suggested to overcome fouling. It was reported that ionic calcium participated in the fouling layer [6,7], and conse-

*Paper presented at the Int Conf on "Engineering of Membrane Processes", Garmisch-Partenkirchen, Germany, May 13–15, 1992

**To whom all correspondence should be addressed

quently its removal by sequestrates, ion exchange resins, dialysis and adjustment of pH followed by centrifugation [8–13] was one of the more successful suggestions for improving fluxes.

Removal of residual fat from the whey is based on the tendency of phospholipoproteins to aggregate under ionic calcium binding, pH change and heat treatment [14]. It was further developed into an industrial process that uses microfiltration (MF) to separate the aggregated mass from the whey, resulting in a clear filtrate that can be further concentrated via UF to produce high quality, fat free WPC [15]. An analysis of the operating parameters of an industrial MF plant was reported by Gésan et al. [16]: permeability and protein transmission were not satisfactory owing to membrane fouling. This fouling was blamed on poor control of the processing variables of the aggregation step (i.e. whey temperature, calcium addition, pH change, heating and holding time) and of the MF operating conditions (i.e. MF temperature and transient operational pathway to stationary permeation flux).

Two variables that are most important for effective MF performance are high flow velocity and low transmembrane pressure (TP) [17,18]. Operating at high flow velocity results in a high pressure drop along the filtering tube, which consequently produces different fluxes along the tube with time [19]. A development patented by Alfa-Laval to overcome the high TP gradient along tubular modules consists in achieving a uniform TP difference throughout the whole length [20–22].

The present work is aimed at acquiring more knowledge about the phenomena that govern membrane fouling during MF of pretreated whey. The influence of fouling evolution with time was studied, and special attention was paid to the role of TP heterogeneity along the membrane. Such studies led us to relate the hydraulic properties of the membrane to the structure and composition of the fouling layers, as analysed by IR and X-ray photoelectron (XPS) spectroscopies.

2. Experimental

2 1 Microfiltration

The MF rig, as described in detail by Daufin et al. [23], was equipped with a single M14 membrane tube (Tech-Sep, Miribel, France), which is a composite membrane made of 0.14 μm mean pore diameter ZrO_2 filtering layer on a carbon support (6 mm inner diameter, 1.2 m long; 2.2×10^{-2} m^2 membrane area). The rig enables MF to be performed in two different modes: static counter pressure mode (SCPM), in which permeate compartment pressure is maintained constant, and dynamic counter pressure mode (DCPM), which consists of circulating the permeate co-current to the retentate in order to create a permeate pressure drop equal to the retentate pressure drop, thus producing no TP difference along the membrane's hydraulic path. Owing to an imperfection of pressure drop regulation with DCPM, MF experiments were performed with a small TP gradient from the inlet of the filtering tube to its outlet, $TP_1 - TP_0 = -0.2$ bar. However, the TP gradient was smaller than that with SCPM (+0.6 bar).

MF was carried out with pretreated whey. Aggregation of residual fat in sweet whey from Emmental cheese was performed by a procedure adapted from that originally proposed by Fauquant et al. [14]: whey at 2°C, plus $CaCl_2$ up to a Ca concentration of 1.2 g-l^{-1} and 10 M NaOH to adjust the pH to 7.2, was heated to 50°C in 30 min, with a holding time of 15 min. The aggregates were separated by MF.

MF experiments, using a new membrane and

a fresh batch of pretreated whey in each operation, were performed at 50±2°C with a mean tangential flow rate (v) of 6.0±0.1 m-sec^{-1} and a mean retentate pressure (P_r) of 4.0±0.1 bar, with an initial pressure drop along the tube of ca. 0.5 bar. The permeation flux (J) was raised to a set value of 64±2 l-hr^{-1}-m^{-2} at a rate of 10 l-hr^{-1}-m^{-2}-min^{-1}, and the stationary volumetric concentration ratio (VCR) was chosen to be 5 by running a feed and bleed system: retentate was extracted as soon as a VCR of 5 had been achieved at the appropriate flow rate as referred to the permeate extraction flow rate. The mean residence time of retained species in the retentate compartment was around 280 min. Operating duration ranged from 1 to 5 hr.

After rinsing the membrane with water, the pure water permeability was assessed by measuring the TP at three levels of J: 20, 40 and 60 l-hr^{-1}-m^{-2} (operating conditions: DCPM, v=4.0 m-sec^{-1}, P_r=1.0 bar, T=50°C). The slope of a plot of J versus TP gave, according to Darcy's law, the hydraulic resistance of the membrane: for a clean membrane R_m, and with irreversible fouling R_{if}. The total fouling R_f, was calculated from TP measured during MF, and reversible fouling R_{rf} as described by Daufin et al. [7].

2.2 Transmission

2.2 1 Analyses

During MF, permeate and retentate samples were withdrawn for analyses of total nitrogen matter (NM), determined according to the Kjeldahl method and expressed as protein (NM×6.38), and of calcium by atomic absorption (Varian SpectrAA 300, Springvale, Australia) as described by Brulé et al. [24]. Transmission ($Tr=100\times C_p/C_r$) was assessed assuming that the permeate compartment was a perfectly stirred reactor [25], and the relative experimental error was evaluated to be ca. 20%. Additional analyses were performed on the feed streams, on the supernatant and on the sediment of centrifuged pretreated whey (2000 g; 15 min; T=30°C) (Table 1): optical density (OD) at 600 nm (Beckman DU 62, Gagny, France); phosphorus, by mineralization and colorimetric determination following the AFNOR norm No NF V 04-284 [26]; α-lactalbumin and β-lactoglobulin by reverse phase high performance liquid chromatography according to a procedure adapted from Jaubert and Martin's work [27]. For the separation, elution was achieved using a linear gradient from 49 to 64% of solvent B for 15 min. Fat content was determined by the method of Folch et al. [28]; proteins, phosphates and lipids were determined by infra-red spectroscopy (see Section 2.3.2) on freeze-dried samples.

TABLE 1

Composition of the feed whey, pretreated whey, supernatant and sediment of centrifuged pretreated whey (2000 g, 15 min, 30°C) (NM total nitrogen matter, α α-lactalbumin, β β-lactoglobulin, Ca calcium, P phosphorus; OD optical density)

	NM	α	β	Lipids (g-l^{-1})	Ca	P	OD
Whey	9 40	0 96	3 69	0 44	0 38	0 42	0 64
Pretreated whey	9 36	0 93	3 80	-	1 30	0 34	1 44
Supernatant	8 54	0 88	3 74	-	0 74	0 18	0 05

Infra-red spectroscopy

	Proteins (mass %)	Lipids (mass %)	Phosphates (mass %)
Sediment	54	18	28

2.2 2 Calculations of "free" protein transmission versus time

The transmission of "free" proteins (not linked to calcium phosphate aggregates [14]) Tr_f, was calculated as follows:

$$Tr_f=\frac{Tr_{exp}-xTr_l}{1-x} \quad (1)$$

where Tr_{exp} is the transmission of total proteins, determined experimentally; Tr_l is the transmission of proteins linked to aggregates, and assumed to be equal to the transmission of aggregated calcium. The concentration of aggregated calcium was determined from the experimental total calcium concentrations and from the percentage of aggregated calcium. The latter was computed using an interative procedure on the *VCR* calculated from a mass balance:

$$VCR=\frac{(1-Tr_{Ca})CF}{1-Tr_{Ca}CF} \tag{2}$$

where Tr_{Ca} = transmission of aggregated calcium (%); CF = concentration factor of aggregated calcium. In eqn. (1), x is the ratio of linked protein concentration to total protein concentration; the linked protein concentration was 1.5 times the concentration of aggregated calcium in the initial pretreated whey. The figure of 1.5 was assumed to be constant throughout the MF run.

2.2.3 Models of selectivity

The analysis of solute and solvent transport through capillaries according to sieving and the Poiseuille flow model allows the calculation of the transmission corresponding to a given membrane pore size [29].

The Poiseuille flow model is considered to correlate solvent flux and pore radius r as follows:

$$J=\frac{TP\times\pi}{8\mu l}r^4 \tag{3}$$

where μ is the dynamic viscosity of the permeate (the solution passing through the pore) and l is the equivalent length of the pore.

The model used for solute transport, taking into account the ratio of molecule radius (r_m) to pore size (as initially proposed by Ferry [30]), was suggested by Munch et al. [31], i.e.:

$$\begin{aligned} &\frac{r_m}{r}<1 \qquad Tr=1-\left[1-\left(1-\frac{r_m}{r}\right)^2\right]^2 \\ &\frac{r_m}{r}>1 \qquad Tr=0 \end{aligned} \tag{4}$$

All types of fouling generate a reduction of the hydraulic permeability of the membrane, which can be attributed to a reduction of the average pore radius [32] determined by the following relationship:

$$r=\left(\frac{R_m}{R}\right)^{0.25}\cdot r_0 \tag{5}$$

where r_0 is the pore radius of the clean membrane; R_m is the membrane hydraulic resistance and R is the fouling hydraulic resistance. From eqn. (5) the reduction of transmission can be evaluated.

The Stokes hydrodynamic radius (r_m) of proteins was calculated from Loret et al. [33] using the following equation:

$$\begin{aligned} r_m=&13.7198-7.6947\ln M \\ &+1.1928(\ln M)^2-0.00717(\ln M)^3 \end{aligned} \tag{6}$$

where M is the molar mass. Table 2 gives the molecular radius calculated from the molar mass for the main four whey proteins, and their concentration in the feed whey needed for the calculation of protein mixture transmission.

TABLE 2

Stokes hydrodynamic radius (r_m) of the four main whey proteins calculated from their molar mass M according to Loret et al [33] (eqn 6) and concentrations of these proteins in the feed whey

	M (Da)	r_m (nm)	C (g·l^{-1})
β-Lactoglobulin	36800	2.8	3.8
α-Lactalbumin	14200	1.8	1.0
Immunoglobulins	600000	7.7	0.6
Bovine serum albumin	66300	3.5	0.3

2.3 Assessment of fouling

2.3.1 Fouling models

The decrease in permeability was modelled according to four filtration laws presented and analysed in relation to the performance of filter media by Grace [34]. The mathematical expressions of these models were established for filtration experiments performed at constant permeation flux.

(i) Filtration in which membrane properties (surface, resistance) do not change in the course of time (t).

The "*cake*" *filtration law*. This model assumes that particles larger than the pores of the medium are retained at the surface of the filter:

$$TP = at + b \tag{7}$$

(ii) Filtration in which membrane properties change during the microfiltration run.

(1) Particles of size around or larger than the pore size of the porous medium.

The "*complete blocking*" *filtration law*. This model assumes that each particle which reaches the membrane participates in the blocking phenomenon by pore sealing. This leads to the assumption that particles are not superimposed:

$$1/TP = ct + d \tag{8}$$

The "*intermediate blocking*" *filtration law*. It is assumed that particles settle on each other. The model evaluates the probability for a particle to block a pore:

$$\ln(TP) = et + f \tag{9}$$

(2) Particles smaller than the pores of the membrane.

The "*standard blocking*" *filtration law*. This model assumes that pore volume decreases proportionally to filtered volume by gradual particle retention and build-up on the pore walls with possible plugging of the pores:

$$(1/TP)^{0.5} = gt + h \tag{10}$$

2.3.2 Analyses of foulants

After membrane rinsing at the conclusion of the MF trial, 3 cm long samples representing the inlet, middle and outlet parts were cut from the 1.20 m long tube. Fouling layers were analysed by two techniques: XPS, which characterizes the surface of the filtering medium, and IR spectrometry; which characterizes the total membrane, surface and bulk.

XPS spectroscopy. XPS measurements were made with an HA 100 hemisphere analyser (VSW, Manchester, UK) placed in an ultra-high vacuum bell (10^{-9}–10^{-10} Torr). The surface under study was exposed to unmonochromatized X-rays from a twin Mg/Al source (1253.6 eV Mg-Kα and/or 1486.6 eV Al-Kα).

The photoelectrons produced are characteristic of the surface; the maximum depth of the analysis is 8–10 nm. Moreover, the appearance of electronic structures of carbon (C1*s*) and nitrogen (N1*s*) was typical of organic fouling. From the area of the peaks that represent each structure profile, the atomic composition could be calculated. The weak cross-section for photoionization of P2*p* explained the difficulty of observing the variations in phosphorus concentration. The calcium signal Ca2$p^{3/2}$ appeared at a binding energy very close to that of Zr3$p^{3/2}$.

The granular form of the Carbosep membrane surfaces prevented direct quantification of the signal intensities of fouling overlayers from electronic emission angle variations. However, in normal incidence, the intensity variation of the zirconium signal (Zr 3*d*) could be measured, and its disappearance indicated a thickness greater than 8–10 nm. A study with an atomic force microscope (AFM, Centre ESCA Université Claude Bernard, Lyon, France) for partly and severely fouled membrane samples confirmed the difficulty in quantifying the fouling thickness (very granular at the beginning and a flattened surface after

heavy fouling, modifying the membrane's topography).

IR spectrometry IR results were computed as mass% of fouled membrane on mean samples that were removed from the active filtering layer which coated the carbon support with a fine spatula, as described by Labbé et al. [6]. The samples comprised the membrane's surface and the internal pore structure of the membrane. The results were referred to as "total fouling". The membranes used in the present experiment are somewhat more complex than the pure tetragonal ZrO_2 found in Carbosep UF membranes [6]. In addition to ZrO_2, they contain titanium oxides that render them a grey colour (greater slope of absorbance vs. wavenumber for blank). The ZrO_2 structure is monoclinic. A new evaluation of the computing program was performed by the standard addition technique, giving a new value: $\epsilon_{ZrO_2}/\epsilon_p = 140$.

3. Results

3.1 Microfiltration with dynamic counter pressure

3.1.1 Evolution of fouling versus time

Normalized overall fouling hydraulic resistances (R_f/R_m) versus time for the four tests performed with the same operating conditions and stopped at various operating times (60, 130, 250 and 320 min) are reported in Fig. 1. The R_m of the membranes ranged from 1.0×10^{12} to 1.3×10^{12} m^{-1}.

The shapes of the curves were quite similar and could be divided into two parts: the first corresponded to a slow increase in R_f/R_m with time; during this period *TP* slowly increased in the range 0.3–0.6 bar, depending on the counter pressure mode and on membrane resistance. The second part showed a much quicker increase of R_f/R_m while the stationary *VCR* was already achieved. *TP* increased from around 1.0 bar to more than 3.0 bar in less than 100 min. Modelling of R_f/R_m for the longest run according to eqns. (7)–(10) exhibited a short initial period of filtration (up to 100 min) during which all models fitted the experimental curves. After 100 min, both the "intermediate blocking" and "cake" filtration laws no longer applied; neither did the "standard blocking" filtration law after 190 min of filtration. The "complete blocking" filtration law was the only model that fitted the curves from the beginning to the end of the MF runs.

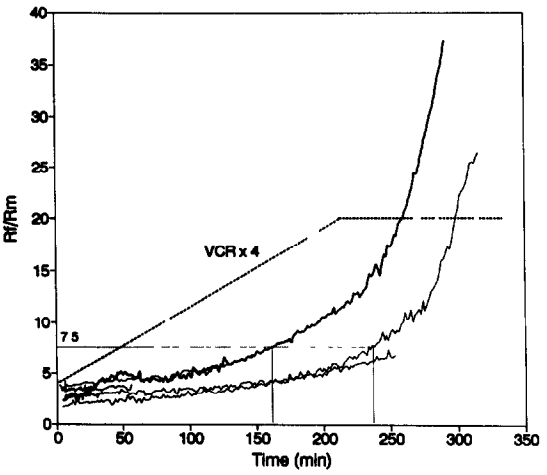

Fig 1 Diagram of normalized overall fouling hydraulic resistance (R_f/R_m) vs time for four experiments performed in static (—) and dynamic (—) counter pressure mode operation ($v=6.0$ m-sec^{-1}, $P_r=4.0$ bar, $T=50°C$, $J=64$ l-hr^{-1}-m^{-2})

The contribution of reversible and irreversible fouling to the total fouling in the course of time is shown in Fig. 2. During the shorter times of operation, reversible fouling R_{rf} contributed more than irreversible fouling R_{if} to the evolution of R_f (60% as compared with 40%). After 250 min of filtration R_{if}/R_m still increased slowly, whereas reversible fouling increased rapidly and became the main contributor to total fouling: $R_{rf}/R_m = 85\%$ of R_f/R_m at the end of the experiment (310 min).

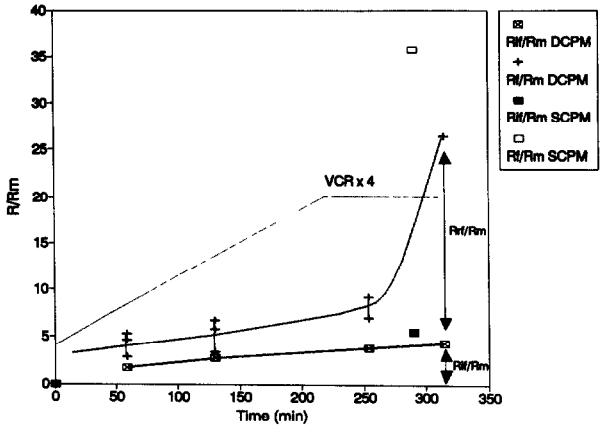

Fig 2 Contribution of reversible (R_{rf}) and irreversible (R_{if}) fouling hydraulic resistances to the development of the overall fouling hydraulic resistance (R_f) referred to membrane resistance (R_m) vs time ($v=6.0$ m-sec^{-1}, $P_r=4.0$ bar, $T=50°C$, $J=64$ l-hr^{-1}-m^{-2}, dynamic counter pressure mode operation, DCPM; static counter pressure mode, SCPM)

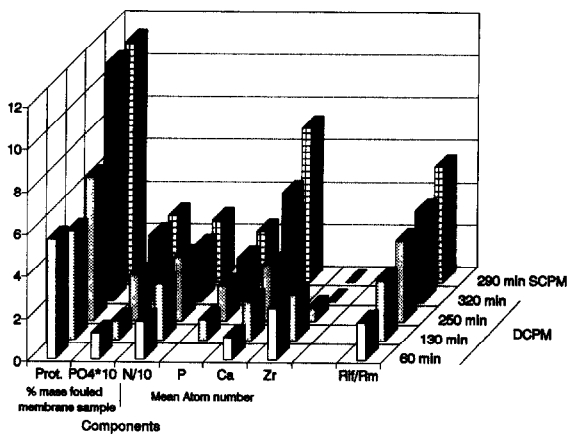

Fig 3 Bar chart of component amounts and normalized irreversible fouling hydraulic resistance (R_{if}/R_m) vs time ($v=6.0$ m-sec^{-1}, $P_r=4.0$ bar; $T=50°C$, $J=64$ l-hr^{-1}-m^{-2}, dynamic counter pressure mode operation, DCPM, static counter pressure mode SCPM)

3.1.2 Analyses of foulants

At the membrane surface (Fig. 3), the disappearance of the Zr signal indicated heavy fouling on the MF membrane (thickness >8–10 nm). The calcium and phosphorus concentrations varied more than proteins (N), indicating the contribution of calcium phosphate clusters to the whey fouling on the surface. This contribution increased as the fouling increased more quickly, since the ratio of protein to phosphate [calculated from N and Ca mass, assuming a $Ca_3(PO_4)_2$ type of phosphate] decreased from about 15 at shorter times down to 3–4 at the end of the MF run. The AFM study confirmed that the fouling covered nearly all the surface (Fig. 4). The higher the fouling, the lower the roughness. The convolution between tip shape and pore shape influenced the apparent pore structures during the profile measurements, increasing the flattened appearance [35].

In the total fouling, as seen by IR spectrometry (Fig. 3), the variation of proteins and phosphates in the course of time did not exactly correspond to the slow increase of irreversible fouling obtained from R_{if}/R_m values, particularly during the last hour of MF, showing their contribution to a great increase of reversible fouling. The mixed material, proteins plus phosphates, exhibited a limited variation of the overall composition expressed as the ratio Prot/PO_4, its mean value being in the region of 50 before 250 min as compared to 30 at the end of MF. In all samples, the phosphates were identified as calcium phosphates (Fig. 5, sample 6). Their structure (Fig. 5) changed in the course of time, as expected for such slowly crystallizing phases. A broad maximum at 1075 cm^{-1}, linked to an amorphous calcium phosphate [36], progressively shifted to 1040 cm^{-1}, showing an apatite phase at the beginning of the crystallization process. This phenomenon was less marked at 320 min, when the withdrawal of retentate for ensuring a stationary *VCR* value of 5 increased the feed flow rate. In the feed and in the retentate, after a few hours' ageing, the aggregates underwent crystallization as apatite, whereas the aqueous phase precipitated as an amorphous calcium phosphate–proteins mixed material. Consequently the intermedi-

ate crystallinity of the apatite observed in the fouling originated from aggregates built up during whey pretreatment and from the remaining ionic calcium and phosphates in the pretreated whey.

3.1.3 Heterogeneity

The distribution of both phosphates and proteins along the tube was far from regular (Fig. 6). The progressive transfer of fouling from the outlet to the inlet of the tube preceded a more pronounced increase of fouling from 250 min. After 320 min, phosphates and proteins reached the same level throughout the tube, with a constant Prot/PO_4 ratio of 30.

3.1.4 MF selectivity

The OD of the permeate at the end of the longer experiment was 0.02, which indicated efficient clarification [37], compared with the initial whey OD of 0.64 (Table 1).

Even though clarification was efficient, transmission of aggregates, as calculated from calcium concentrations, was estimated at 5% throughout the experiment. The transmission of calcium, which took into account ionic and precipitated calcium originating from calcium phosphate aggregation (produced during whey pretreatment), decreased during the first 200 min from 40% down to a plateau at 20% (Fig. 7).

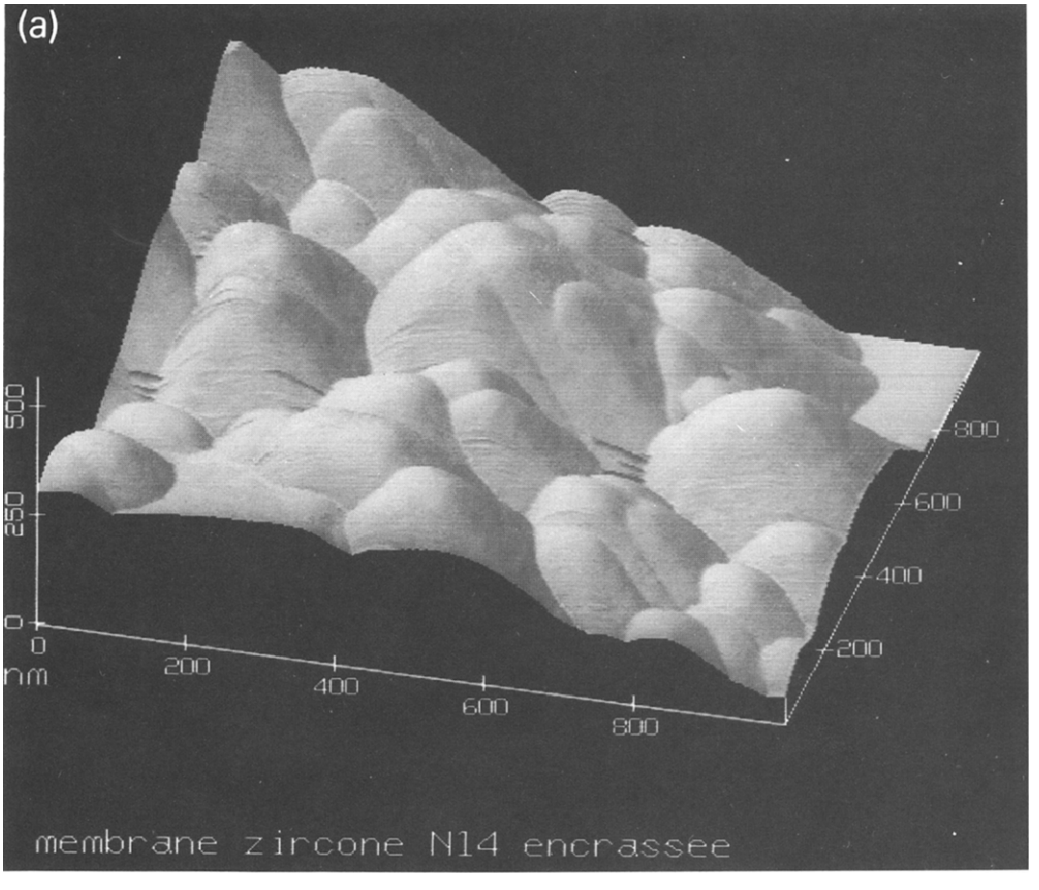

Fig 4 Atomic force microscope image of the surface of an M14 membrane fouled with pretreated whey (a) after 60 min of fouling in dynamic counter pressure mode operation (DCPM), (b) after 320 min of fouling in DCPM

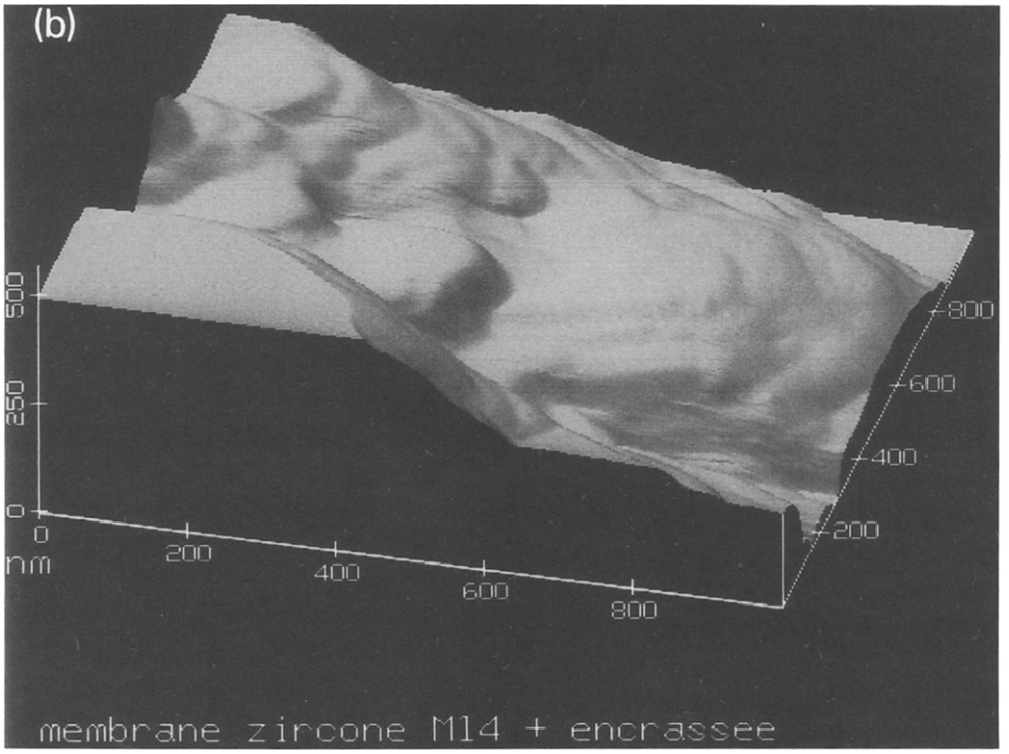

During the slow increase of fouling (up to 130 min), the protein transmission decreased from 70 to ca. 60% (Fig. 7). After about 210 min of filtration, when more rapid increase of reversible fouling occurred, transmission of proteins to the permeate compartment decreased sharply down to 30% (Fig. 7).

3.2 Comparison between static (SCPM) and dynamic (DCPM) counter pressure mode

Despite the difference between SCPM and DCPM, the curves of the overall hydraulic resistance (R_f/R_m) vs. time were quite similar (Fig. 1). Nevertheless, crossflow microfiltration performed using DCPM resulted in slower irreversible (R_{if}/R_m) and reversible (R_{rf}/R_m) fouling compared with SCPM (Fig. 2). As a consequence, operating time before severe fouling occurred was longer. For instance, the time to reach an R_f/R_m value of 7.5 was 50% longer than that in SCPM (Fig. 1).

At the end of the filtration in either mode, Zr became totally masked (Fig. 3) owing to a fouling layer thicker than 8–10 nm. The homogeneity along the tube and the nature of the surface irreversible layer were similar in both modes of operation, and the number of atoms measured was higher in SCPM compared to DCPM. Given that the thickness of the irreversible fouling layer revealed by the XPS analyses was constant for the different experiments, and that *TP* was lower at the end of the experiment performed in DCPM (compared with SCPM), it is likely that the irreversible fouling layer was less compressed.

No difference was detected in the total fouling: the same mean values for proteins and

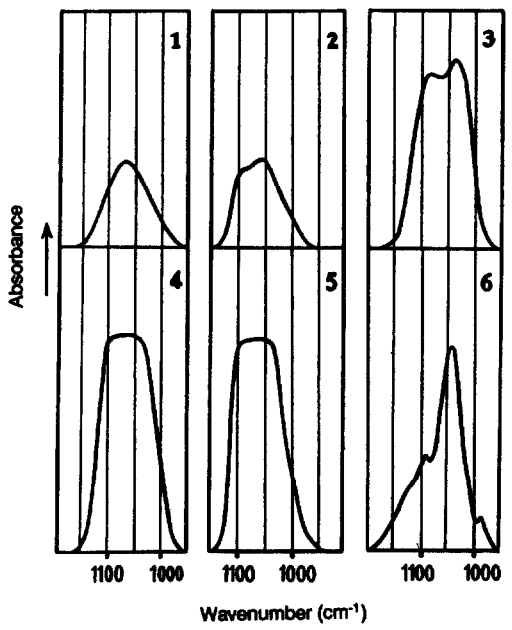

Fig 5 Absorbance vs. wavenumber for comparable amounts of fouled M14 membrane ($155 \pm 10\,\mu g$) taken in the middle of the tube ($v=6.0$ m-sec^{-1}, $P_r=4.0$ bar, $T=50$°C, $J=64$ l-hr^{-1}-m^{-2}) Curve 1, 60 min MF at dynamic counter pressure (amorphous profile), curve 2, 130 min, curve 3, 250 min, curve 4, 320 min Curve 5, 290 min MF at static counter pressure Curve 6, sample 3 heated at 600°C (recrystallized apatite profile)

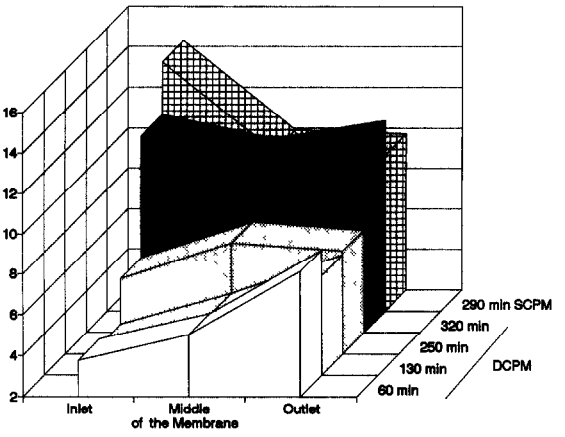

Fig. 6 Bar chart of protein amounts (expressed as mass % of fouled membrane sample) at the inlet, middle and outlet of the membrane tube vs time for experiments performed in dynamic (DCPM) and static (SCPM) counter pressure mode operation ($v=6.0$ m-sec^{-1}, $P_r=4.0$ bar, $T=50$°C, $J=64$ l-hr^{-1}-m^{-2})

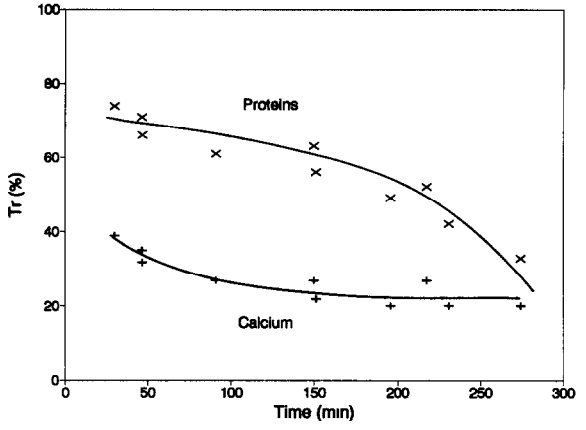

Fig 7 Diagram of protein and calcium transmission (Tr) into the permeate compartment vs time ($v=6.0$ m-sec^{-1}, $P_r=4.0$ bar, $T=50$°C, $J=64$ l-hr^{-1}-m^{-2}, dynamic counter pressure mode operation)

phosphates, the same Prot/PO_4 ratio (Fig. 3) and similar calcium phosphate structures (nearly amorphous) (Fig. 5) were observed. Nevertheless, the fouling distribution along the tube at the end of the MF run was quite different (Fig. 6): no variation was observed with DCPM, whereas with SCPM a regular decrease of fouling existed from the inlet to the outlet and was greater for phosphates than for proteins. Protein transmission was 5% lower with SCPM, a trend that was shown to be amplified at higher permeation fluxes [38]. As a consequence of lower fouling with DCPM, the recovery of protein when R_f/R_m reached 7.5 was 67%, compared to 58% with SCPM.

4. Discussion

4.1 MF performance; TP heterogeneity

Besides the good efficiency of clarification, it is noteworthy that protein transmission was insufficient: around 30% at the end of the MF experiments. The figures were of the same or-

der of magnitude as those found for an industrial plant [16].

Even though protein transmission was not improved much with DCPM, the enhancement of operating time could be explained by a lower overall fouling, which could be related to a more even *TP* distribution from the inlet to the outlet of the membrane tube. A striking difference between SCPM and DCPM was the distribution of fouling along the tube. With both modes of operation, a *TP* gradient ($TP_1 - TP_0$) appeared, which was higher in SCPM ($TP_1 - TP_0 = +0.6$ bar) than in DCPM (negative *TP* gradient; $TP_1 - TP_0 = -0.2$ bar). As a result, fouling was more evenly distributed with DCPM as compared to SCPM. At shorter times of operation using DCPM, fouling was higher in regions subject to a higher pressure difference. As a consequence, the less fouled areas under lower transmembrane pressure were forced to filter bigger volumes. Therefore they fouled more rapidly, so the fouling layer was evenly distributed by the end of the MF run. These results considered a movement of the effective filtering area on a macroscopic scale, which should be confirmed in a further study performed at SCPM under a higher pressure gradient.

It should be noted that Riesmeier et al. [17] observed such a heterogeneity of local filtering conditions and fouling with crossflow MF of microbial cells. The authors called for more attention to be focussed on the module construction in order to lower the pressure drop in the retentate side. From our work it appears that DCPM is an adequate system for overcoming this obstacle.

4.2 Contribution of aggregates and proteins to fouling

The "complete blocking" filtration law was the only model that fitted the experimental data throughout the experiment. It exhibited the influence of reduction of filtering area by particles, which revealed the role of aggregates. They accumulated at the membrane surface and penetrated into pores, particularly during the last hour, when the reduction of filtering area led to a major increase of J per remaining active surface area (the experiments were performed at constant J). The aggregates formed during the pretreatment given to the whey were the principal source of calcium phosphates, which had a tendency to crystallize as apatite. Nevertheless, the remaining ionic calcium and phosphate might precipitate during the MF operation owing to the operating conditions: the same temperature as that of pretreatment (50°C); the pH of the feed (6.5) and of the retentate (6.4) after 190 min; the mean residence time in the feed tank and retentate compartment (280 min). Hickey and Hill [39] observed that UF pore blocking can occur more severely if apatite is permitted to form in the whey during a run rather than before it. This kind of inorganic foulant is known to cause a severe decline of membrane permeability in UF of raw whey [7,40].

Nevertheless, according to spectroscopic analyses, proteins linked to aggregates and in a "free" state were the major foulant. "Free" proteins were dominant, since the ratio Prot/PO_4 exceeded 30 (Fig. 3), which is much higher than in the aggregates, where the ratio was around 2 (proteins 54%, phosphates 28%, lipids 18% as determined by IR spectrometry). Their content was particularly high at the surface and in the bulk of the membrane relative to results found in the ultrafiltration of clarified whey, despite the lower specific membrane area of MF membranes (2 $m^2 \cdot g^{-1}$ for M14) compared with UF (48 $m^2 \cdot g^{-1}$ for M5) [6,7].

"Free" proteins and aggregates participated in a reversible cake build-up and in the irreversible fouling. During microfiltering, the reduction of filtering area induced an enhanced transfer of proteins and aggregates towards the

remaining filtering area. Then proteins were captured by a more concentrated and compressed cake under a higher TP and by the irreversibly fouled membrane. Such phenomena resulted in a decrease of protein concentration in the permeate compartment when R_{rf} increased.

4.3 Selectivity

In the course of the MF operation, retention of proteins linked to calcium phosphate aggregates could not entirely explain the low total protein transmission. Therefore "free" protein transport through the filtering layer was altered by increased fouling.

According to Ferry's law [30] the clean M14 membrane with a mean pore diameter of 0.14 μm and a hydraulic resistance of R_m should readily transmit the main "free" whey proteins (Table 3). The calculated transmission of total proteins (linked and "free" proteins) was estimated to be 90%.

At shorter filtration times, the increase of hydraulic resistance due to irreversible fouling (R_m+R_{if}) led to a reduction of the membrane pore radius (down to 0.048 μm after 4 hr), which did not contribute significantly to the development of protein transmission: pores were still large enough to enable passage of protein through the membrane. The same conclusion was reached with the reduction of pore radius due to the irreversible fouling (R_m+R_{if}) for longer operating times.

The overall fouling hydraulic resistance (R_m+R_f) was insufficient to account for a total protein transmission of 30%, even with its higher level at the end of the MF run (Table 3).

Consequently, the large discrepancy between experimental and modelled Tr values inclines one to reconsider the relevance of the assumptions made with respect to membrane fouling models: fouling is assumed to cause reduction of pore size when using Ferry's and Poiseuille's laws (eqn. (5), [32]), while pores becoming blocked and sealed are supposed to account for the development of fouling in the MF experiments. Moreover, the heterogeneity of the system, which involves the development of fouling from the inlet to the outlet of the membrane, at the surface and in the bulk of the membrane as well as changes in pore size distribution with time [29,41], emphasizes the complexity of the fouling phenomena that have to be taken into account. The phenomenon of protein retention by MF membranes with pore sizes bigger than the proteins was reported [42–44]. It was explained for whey protein by the interaction of charged molecules with charges on the membrane [42] and for bovine serum albumin solution by the effect of shear on the protein molecules being sufficient to expose hydrophobic groups, which have a higher tendency to adsorb onto membranes and to induce aggregation of the more denatured form of protein [45].

According to the above, we suggest that more attention should be paid to the distribution of protein transmission along the membrane in the course of time, to the contribution of each

TABLE 3

Protein transmission determined experimentally (Tr_{exp}) and calculated from Poiseuille's (eqn (5)) and Ferry's (eqn (4)) laws (Tr_{model}) at various MF times taking into account different values of fouling hydraulic resistance R

R	Time (min)	Pore radius (nm)	Tr_{model} (%)	Tr_{exp} (%)
R_m	0	70	90	-
R_m+R_{if}	60	54	81	-
	130	50	77	-
	250	48	64	-
	320	46	64	-
R_m+R_f	60	45	80	66
	130	42	76	60
	250	42	73	40
	320	30	72	30

individual protein to the fouling and to protein retention during MF. For instance, the role of charge effects and protein–protein, protein–particle, protein–membrane interactions, as well as membrane characteristics and pore microstructure, should be further investigated.

5. Conclusions

In pretreated whey MF, calcium phosphate aggregates and proteins were responsible for heterogeneous fouling that increased in the course of time according to a "complete blocking" filtration law accounting for a progressive decrease in the active filtering area, which moved along the membrane from the higher to the lower transmembrane pressure areas.

The dynamic counter pressure mode of operation provides a nearly constant transmembrane pressure gradient along the filtering module. Consequently, it is a precious scientific tool for investigating fouling phenomena. Moreover, it is an efficient means for improving the performance of MF systems, giving longer operating time and higher protein recovery.

The development of protein transmission in the course of time is not completely understood, and knowledge concerning the influence of microscopic heterogeneity (distribution of pore size, etc.) and of membrane–solute interactions need to be improved.

Acknowledgements

This work was supported by a grant from the Etablissement Public Régional Bretagne (Contract No. 3051 B). The authors gratefully acknowledge the valuable contribution of F.-L. Kerhervé and J.-F. Radenac in building the counter pressure system.

List of symbols

a,b,c,d,e,f,g,h	constants of eqns. (7)–(10)
C	protein concentration ($g\text{-}l^{-1}$)
CF	concentration factor of aggregated calcium
C_p	permeate concentration ($g\text{-}l^{-1}$)
C_r	retentate concentration ($g\text{-}l^{-1}$)
J	permeation flux ($m^3\text{-}m^{-2}\text{-}sec^{-1}$ or $l\text{-}hr^{-1}\text{-}m^{-2}$)
l	equivalent length of the membrane pore (m)
M	molar mass ($g\text{-}mol^{-1}$ or Da)
OD	optical density
P_r	mean retentate pressure (Pa or bar)
r	pore radius (m or nm)
r_m	molecular radius (m or nm)
r_0	pore radius of the clean membrane (m or nm)
R	fouling hydraulic resistance (m^{-1})
R_f	overall fouling hydraulic resistance (m^{-1})
R_{if}	irreversible fouling hydraulic resistance (m^{-1})
R_m	membrane hydraulic resistance (m^{-1})
R_{rf}	reversible fouling hydraulic resistance (m^{-1})
t	time (sec or min)
TP	transmembrane pressure (Pa or bar)
TP_i, TP_o	transmembrane pressure at the inlet and at the outlet of the filtering tube (Pa or bar)
Tr	transmission (%)
Tr_{Ca}	transmission of aggregated calcium (%)
Tr_{exp}	protein transmission determined experimentally (%)
Tr_f	transmission of "free" proteins not linked to calcium phosphate aggregates (%)

Tr_1	transmission of proteins linked to calcium phosphate aggregates (%)
Tr_{model}	protein transmission calculated from Poiseuille's (eqn. (4)) and Ferry's (eqn. (5)) laws (%)
v	mean tangential flow rate (m sec^{-1})
VCR	volumetric concentration ratio
x	ratio of linked protein concentration to total protein concentration
ϵ_{ZrO_2}, ϵ_p	molecular extinction coefficient for zirconium oxide ZrO_2 and protein p
μ	dynamic viscosity of the permeate (Pa-sec)

References

1 J E Kinsella, Functional properties of proteins in foods A survey, CRC Crit Rev Food Sci Nutr, 4 (1976) 219
2 K.R. Marshall and W J Harper, Whey protein concentrates, Int Dairy Fed Bull, 233 (1988) 21
3 C V Morr and E.A Foegeding, Composition and functionality of commercial whey and milk protein concentrates and isolates a status report, Food Technol, 43 (1990) 100
4 S H Richert, C V Morr and C M Cooney, Effect of heat and other factors upon foaming properties of whey protein concentrates, J Food Sci, 39 (1974) 42
5 R J Pearce, S C Marshall and J A Dunkerley, Reduction of lipids in whey protein concentrates by microfiltration, Int Dairy Fed Special Issue, 9201 (1992) 118
6 J.-P Labbé, A Quémerais, F Michel and G Daufin, Fouling of inorganic membranes during whey ultrafiltration analytical methodology, J Membrane Sci, 51 (1990) 293
7 G Daufin, J -P Labbé, A. Quémerais and F Michel, Fouling of an inorganic membrane during ultrafiltration of defatted whey protein concentrates, Neth Milk Dairy J, 45 (1991) 259
8 D N Lee and R L Merson, Chemical treatment of cottage cheese whey to reduce fouling of ultrafiltration membranes, J Food Sci, 41 (1976) 778
9 U Merin and M Cheryan, Factors affecting the mechanism of flux decline during UF of cottage cheese whey, J Food Process Preserv, 4 (1980) 183
10 B M Ennis, J E M Johns and M T O'Connell, The effect of the replacement of calcium with sodium on the ultrafiltration of acid whey, N Z J Dairy Sci Technol, 16 (1981) 69
11 K P Kuo and M Cheryan, Ultrafiltration of acid whey in a spiral-wound unit effect of operating parameters on membrane fouling, J Food Sci, 48 (1983) 1113
12 J Patoka and P Jelen, Calcium chelation and other pre-treatments for flux improvement in ultrafiltration of cottage cheese whey, J Food Sci, 52 (1987) 1241
13 C Taddéi, Mécanismes influençant le transfert de matière lors de l'ultrafiltration de lactosérum, Thesis, Toulouse University, 1986
14 J Fauquant, S Vieco, G Brulé and J -L Maubois, Clarification des lactosérums doux par agrégation thermocalcique de la matière grasse résiduelle, Lait, 65 (1985) 1
15 J -L Maubois, A Pierre, J Fauquant and M Piot, Industrial fractionation of main whey proteins, Int Dairy Fed Bull, 212 (1987) 154
16 G Gésan, U Merin, G Daufin and J -J Maugas, Performance of an industrial microfiltration plant for clarifying rennet whey, Neth Milk Dairy J, submitted (1992).
17 B Riesmeier, K H Kroner and M -R Kula, Studies on secondary layer formation and its characterization during cross-flow filtration of microbial cells, J Membrane Sci, 34 (1987) 245
18 M Piot, J C Vachot, M Veaux, J -L Maubois and G E Brinkman, Ecrémage et épuration bactérienne du lait entier cru par microfiltration sur membrane en flux tangentiel, Tech Lait Market, 1016 (1987) 42
19 U Merin and G Daufin, Crossflow microfiltration in the dairy industry state-of-the-art, Lait, 70 (1990) 281
20 R M Sandblom (Alfa-Laval), Filtering Process, Swedish Patent No 7,416,257 (1974)
21 M Malmberg and S Holm, Low bacteria skim milk by microfiltration, North Eur Food Dairy J, 54 (1988) 75
22 E Plett, The constant pressure difference method for microfiltration, in H G Kessler and D B Lund (Eds), Fouling and Cleaning in Food Processing, 1989, p 283
23 G Daufin, J -F Radenac, G Gésan, F -L Kerhervé, F Michel, U Merin and O Le Berre, A novel rig for ultra- and microfiltration for separating milk and whey components, Sep Sci Technol, submitted (1992)
24 G Brulé, J -L Maubois and J Fauquant, Etude de la teneur en éléments minéraux des produits obtenus lors de l'ultrafiltration du lait sur membrane, Lait, 54 (1974) 600

25 T Courtois, M. Mietton-Peuchot and A Davin, Etude expérimentale de la formation de la couche de polarisation, 3ème Congrès Français de Génie des Procédés, Compiègne, Lavoisier, Vol 5, 1991, p 73

26 AFNOR-ITSV, Contrôle de la qualité des produits laitiers Recueil des normes françaises, S Amariglio (Ed), 3rd edn , 1986

27 A Jaubert and P Martin, Reverse-phase HPLC analysis of goat caseins Identification of α_{s1} and α_{s2} genetic variants, Lait, 72 (1992) 235

28 J Folch, M Lees and G A Sloane-Stanley, A simple method for isolation and purification of total lipids from animal tissues, J Biol Chem , 266 (1957) 497

29 P Aimar, M Meireles and V Sanchez, A contribution to the translation of retention curves into pore size distributions for sieving membranes, J Membrane Sci , 54 (1990) 321

30 J D Ferry, Ultrafilter membranes and ultrafiltration, Chem Res , 18 (1936) 376

31 W D Munch, L P Zestar and J L Anderson, Rejection of polyelectrolytes from microporous membranes, J Membrane Sci , 5 (1979) 77

32 L Zeman, Adsorption effects in retention of macromolecules by ultrafiltration membranes, J Membrane Sci , 15 (1983) 213

33 C Loret, B Chaufer, B Sebille, M Hanselin, Y Blain and A Le Hir, Characterization and hydrodynamic behaviour of modified gelatin II Characterization by high performance size exclusion chromatography—comparison with dextrans and proteins, Int J Biol Macromol , 10 (1988) 366

34 H P Grace, Structure and performance of filter media, AIChE J , 2 (1956) 307

35 P Dietz, P K Hansma, O Inacker, H -D Lehmann and K -H Herrmann, Surface pore structures of micro- and ultrafiltration membranes imaged with the atomic force microscope, J Membrane Sci , 65 (1992) 101

36 M Dupeyrat, J -P Labbé, F Michel, G Daufin and F Billoudet, Mouillabilité et interactions solide–liquide dans l'encrassement de divers matériaux par du lactosérum et du lait, Lait, 67 (1987) 465

37 A Pierre, Y Le Graet, J Fauquant, C Durier and A Kobilinski, Evaluation du rôle des paramètres physico-chimiques dans la clarification du lactosérum, Lait, 72 (1992) 405

38 G Gésan, G Daufin, U Merin, F Michel, F -L Kerhervé and J -F Radenac, Colmatage d'une membrane inorganique de microfiltration par du lactosérum, in G Antonini and R Ben Aim (Eds), 3ème Congrès Français de Génie des Procédés, Compiègne, Lavoisier, Vol 5, 1991, p 19

39 M W Hickey and R D Hill, Investigations into the ultrafiltration and reverse osmosis of wheys II The effects of some minor whey constituents, N Z J Dairy Sci Technol , 15 (1980) 123

40 C Taddei, G Daufin, P Aimar and V Sanchez, Role of some whey components on mass transfer in ultrafiltration, Biotechnol Bioeng , 34 (1989) 171

41 J Hubble, Modelling of protein rejection by microfiltration membranes, in H G Kessler and D B Lund (Eds), Fouling and Cleaning in Food Processing, 1989, p 239

42 P Heineman, J A Howell and R A Bryan, Microfiltration of protein solutions effects of fouling on rejection, Desalination, 68 (1988) 243

43 V Gekas and B Hallstrom, Microfiltration membranes, cross-flow transport mechanisms and fouling studies, Desalination, 77 (1990) 195

44 H C Van Der Horst, Microfiltration in whey processing, in J Charpin and L Cot (Eds), First Int Conf Inorganic Membranes, Montpellier, 3–6 June 1989, p 297

45 A C M Franken, J T M Sluys, V Chen, A G Fane and C J D Fell, Role of protein conformation on membrane characteristics, 5th World Filtration Congr , Nice, 5–8 June 1990, Société Française de Filtration, Cachan, Vol 1, p 207